

Virtual Hadronic and Leptonic Contributions to Bhabha Scattering

Stefano Actis,¹ Michał Czakon,^{2,3} Janusz Gluza,³ and Tord Riemann⁴

¹*Institut für Theoretische Physik E, RWTH Aachen, D-52056 Aachen, Germany*

²*Institut für Theoretische Physik und Astrophysik,*

Universität Würzburg, Am Hubland, D-97074 Würzburg, Germany

³*Institute of Physics, University of Silesia, Uniwersytecka 4, PL-40007 Katowice, Poland*

⁴*Deutsches Elektronen-Synchrotron, DESY, Platanenallee 6, D-15738 Zeuthen, Germany*

Using dispersion relations, we derive the complete virtual QED contributions to Bhabha scattering due to vacuum polarization effects in photon propagation. We apply our result to hadronic corrections and to heavy lepton and top quark loop insertions. We give the first complete estimate of their net numerical effects for both small and large angle scattering at typical beam energies of meson factories, LEP, and the ILC. The effects turn out to be smaller, in most cases, than those corresponding to electron loop insertions, but stay, with amounts of typically one per mille, of relevance for precision experiments. Hadronic corrections themselves are typically about 2–3 times larger than those of intermediate muon pairs (the largest heavy leptonic terms).

PACS numbers: 11.15.Bt, 12.20.Ds

The determination of the luminosity at lepton and hadron colliders is a necessary task, since in many cases the normalization of the measured cross sections is an observable of direct phenomenological interest. In practice, this task can only be solved by selecting a particular reference process, which is expected to generate large statistics, be as free as possible of systematic ambiguities and predicted by the theory to suitable accuracy. As far as lepton colliders are concerned, the above criteria are fulfilled by Bhabha scattering, i.e. the $e^+e^- \rightarrow e^+e^-$ process, where a precision under the per mille level can be achieved on both the theory and the experimental sides.

In the last few years, there has been major progress in the evaluation of the corrections at the next-to-next-to-leading order accuracy. In fact, the two-loop QED corrections were first evaluated in the massless case in [1]. The photonic corrections to massive Bhabha scattering with enhancing powers of $\ln(s/m_e^2)$ were soon derived from that [2]. The missing constant term [3] plus the corrections with electron loop insertions [4, 5] followed much later. Recently, the heavy fermion (or $N_f = 2$) corrections were derived in the limit $m_e^2 \ll m^2 \ll s, |t|, |u|$ [5, 6], where m is the mass of the heavy fermion, and soon after also for $m_e^2 \ll m^2, s, |t|, |u|$ [7, 8].

In this letter, we present the last missing part of the virtual corrections, the hadronic ones, and argue that the new contribution is of relevance for present and future experiments.

The three main classes of diagrams that we consider are shown in Fig. 1. They may be evaluated by dispersion integrals, after replacing the vacuum polarization insertion $\Pi_{\text{had}}(q^2)$ (we discuss the hadronic case explicitly, and make reference to the heavy fermion case later) to the photon propagator [9],

$$\frac{g_{\mu\nu}}{q^2 + i\delta} \rightarrow \frac{g_{\mu\alpha}}{q^2 + i\delta} (q^2 g^{\alpha\beta} - q^\alpha q^\beta) \Pi_{\text{had}}(q^2) \frac{g_{\beta\nu}}{q^2 + i\delta}, \quad (1)$$

by the once-subtracted dispersion integral

$$\Pi_{\text{had}}(q^2) = -\frac{q^2}{\pi} \int_{4M_\pi^2}^{\infty} \frac{dz}{z} \frac{\text{Im} \Pi_{\text{had}}(z)}{q^2 - z + i\delta}. \quad (2)$$

Finally, one relates $\text{Im} \Pi_{\text{had}}$ to the hadronic cross-section ratio R_{had} ,

$$\text{Im} \Pi_{\text{had}}(z) = -\frac{\alpha}{3} R_{\text{had}}(z) = -\frac{\alpha}{3} \frac{\sigma_{e^+e^- \rightarrow \text{hadrons}}(z)}{(4\pi\alpha^2)/(3z)}, \quad (3)$$

measured experimentally in the low-energy region and around hadronic resonances, and given by the perturbative QCD prediction elsewhere. For heavy fermion insertions, we have $R_f = Q_f^2 C_f (1 + 2m_f^2/z) \sqrt{1 - 4m_f^2/z}$ (with electric charge Q_f and color factor C_f) to leading order, which is sufficient for practical purposes. For leptonic or top quark intermediate states the dispersion relation approach is just an efficient technique of evaluation, but it becomes essential for light quark loops. In the case of Bhabha scattering, this method was first used some time ago for (one-loop) propagator insertions [10]. It was also applied to two-loop irreducible vertex (plus soft real pair) corrections [11]. Here, we derive semi-analytical cross section formulae for the so far unknown hadronic box diagrams (see Fig. 1c). In the numerical results, however, the three classes of contributions will be discussed together.

After replacing the photonic self energy insertion in a two-loop diagram by the integral (2) and subsequently interchanging loop and dispersion integrations, one arrives at effective, massive one-loop Feynman integrals in the kernels, $K(z)$, of the dispersion integrals (details of the evaluation will be presented elsewhere). Whereas the single vertex kernel K_v can be found in Eq. (5) of [11], the cross section corrections due to the double boxes of Fig. 1c depend on three such kernels $K_a(z)$, $a = A, B, C$ [8] [18]. Notice that unlike the vertex kernel, the box

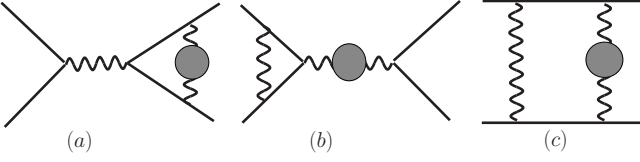


FIG. 1: Three classes of virtual hadronic Bhabha diagrams. (a) and (b) represent hadronic irreducible and reducible vertex diagrams, (c) irreducible hadronic box diagrams.

kernels are infrared divergent:

$$K_a(x, y, z) = \frac{2v_a(x, y)}{3(y - z)} \left(\frac{1}{\epsilon} + L_{-s} \right) L_x \quad (4)$$

$$+ \sum_{w=x, y, z} C_{a2}^w(x, y, z) L_w^2 + \dots,$$

where x, y may be s, t, u , the $L_w = \ln(-w/m_e^2)$, and with Born factors $v_A = (x + y)^2$, $v_B = (2x^2 + y^2 + 2xy)$, and $v_C = v_A - v_B$. The net cross section contribution from the eight double box diagrams has the structure:

$$\frac{d\sigma_B}{d\Omega} = c \Re \int_{4M_\pi^2}^{\infty} dz \frac{R_{\text{had}}(z)}{z} \left\{ \frac{1}{t - z} I_1(s, t; z) \right. \quad (5)$$

$$+ \frac{1}{s - z} \left[I_2(s, t; z) + I_3(s, t; z) \ln \left(1 - \frac{z}{s} \right) \right] \Big\}$$

$$+ c \pi \Im \int_{4M_\pi^2}^{\infty} dz \frac{R_{\text{had}}(z)}{z} \frac{1}{s - z} I_3(s, t; z),$$

with $c = (\alpha/\pi)^2 \alpha^2/s$, and where $s \rightarrow s + i\delta$ if necessary. Two of the double box cross section functions $I_i(s, t; z)$ are infrared divergent, but, analogously to the one-loop case, they have no mass singularity:

$$I_1(s, t, z) = - \left[\frac{1}{\epsilon} + \ln \left(\frac{z}{s} \right) \right] c(s, t) \ln \left[-\frac{u}{s} \right] + \dots, \quad (6)$$

with $c(s, t) = [v_A(s, t)/s + v_B(s, t)/t]/3$, and for $I_2(s, t, z)$ the s and t are interchanged in the divergent part (for

details see [12]). The result becomes infrared finite after combining the double box terms with single box diagrams (interfering with Born diagrams containing self energy insertions) and with initial-final state (or electron-positron line) interferences of real radiation diagrams (one of them containing a self energy insertion). In the following, we will also add the $N_f = 2$ reducible one- and two-loop vertex corrections (building an infrared finite subset together with interferences of initial or final state and of electron or positron real photon emission contributions), thus combining *all* the infrared divergent terms together. In other words, we only exclude from this part the $N_f = 2$ irreducible vertices and pure self energies. The result becomes for $0 < s < 4M_\pi^2$:

$$\frac{d\bar{\sigma}}{d\Omega} = c \int_{4M_\pi^2}^{\infty} dz \frac{R_{\text{had}}(z)}{z} \left\{ \frac{1}{t - z} F_1(z) \right. \quad (7)$$

$$+ \frac{1}{s - z} \left[F_2(z) + F_3(z) \ln \left(\frac{z}{s} - 1 \right) \right] \Big\}.$$

For $s > 4M_\pi^2$, we have performed the necessary analytical continuations and parametrize the outcome by four functions $F_i(z)$:

$$\frac{d\bar{\sigma}}{d\Omega} = c \int_{4M_\pi^2}^{\infty} dz \frac{R_{\text{had}}(z)}{z} \frac{1}{t - z} F_1(z) \quad (8)$$

$$+ c \int_{4M_\pi^2}^{\infty} \frac{dz}{z(s - z)} \left\{ R_{\text{had}}(z) \left[F_2(z) + F_3(z) \ln \left| 1 - \frac{z}{s} \right| \right] \right.$$

$$- R_{\text{had}}(s) \left[F_2(s) + F_3(s) \ln \left| 1 - \frac{z}{s} \right| \right] \Big\}$$

$$+ c \frac{R_{\text{had}}(s)}{s} \left\{ F_2(s) \ln \left(\frac{s}{4M_\pi^2} - 1 \right) - 6\zeta_2 F_4(s) \right.$$

$$+ F_3(s) \left[2\zeta_2 + \frac{1}{2} \ln^2 \left(\frac{s}{4M_\pi^2} - 1 \right) + \text{Li}_2 \left(1 - \frac{s}{4M_\pi^2} \right) \right] \Big\}.$$

The net cross section kernel functions for the selected set of diagrams are:

$$F_1(z) = \frac{1}{3} \left\{ 9c(s, t) \ln \left(\frac{s}{m_e^2} \right) + \left[-z^2 \left(\frac{1}{s} + \frac{2}{t} + 2 \frac{s}{t^2} \right) + z \left(4 + 4 \frac{s}{t} + 2 \frac{t}{s} \right) + \frac{1}{2} \frac{t^2}{s} + 6 \frac{s^2}{t} \right. \right.$$

$$+ 5s + 4t \Big] \ln \left(-\frac{t}{s} \right) + s \left(-\frac{z}{t} + \frac{3}{2} \right) \ln \left(1 + \frac{t}{s} \right) + \left[\frac{1}{2} \frac{z^2}{s} + 2z \left(1 + \frac{s}{t} \right) - \frac{11}{4} s - 2t \right] \ln^2 \left(-\frac{t}{s} \right)$$

$$- \left[\frac{1}{2} \frac{z^2}{t} - z \left(1 + \frac{s}{t} \right) + \frac{t^2}{s} + 2 \frac{s^2}{t} + \frac{9}{2} s + \frac{15}{4} t \right] \ln^2 \left(1 + \frac{t}{s} \right) + \left[\frac{z^2}{t} - 2z \left(1 + \frac{s}{t} \right) + 2 \frac{s^2}{t} + 5s + \frac{5}{2} t \right]$$

$$\times \ln \left(-\frac{t}{s} \right) \ln \left(1 + \frac{t}{s} \right) - 4 \left[\frac{t^2}{s} + 2 \frac{s^2}{t} + 3(s + t) \right] \left[1 + \text{Li}_2 \left(-\frac{t}{s} \right) \right] - \left[\frac{t^2}{s} + 2 \frac{s^2}{t} + 3(s + t) \right] \ln \left(\frac{z}{s} \right) \ln \left(1 + \frac{t}{s} \right)$$

$$- \left[2 \frac{z^2}{t} - 4z \left(1 + \frac{s}{t} \right) - 4 \frac{t^2}{s} - 2 \frac{s^2}{t} + s - \frac{11}{2} t \right] \zeta_2 + \left[z^2 \left(\frac{1}{s} + 2 \frac{s}{t^2} + \frac{2}{t} \right) - z \left(\frac{t}{s} + 2 \frac{s}{t} + 2 \right) \right] \ln \left(\frac{z}{s} \right)$$

$$- \left[z^2 \left(\frac{1}{s} + \frac{1}{t} \right) + 2z \left(1 + \frac{s}{t} \right) + s + 2 \frac{s^2}{t} \right] \ln \left(\frac{z}{s} \right) \ln \left(1 + \frac{z}{s} \right) + \left[\frac{z^2}{s} + 4z \left(1 + \frac{s}{t} \right) - \frac{t^2}{s} - 4(s + t) \right]$$

$$\begin{aligned}
& \times \ln\left(\frac{z}{s}\right) \ln\left(1 - \frac{z}{t}\right) - \left[z^2 \left(\frac{1}{s} + 2\frac{s}{t^2} + \frac{2}{t} \right) - 2z \left(\frac{t}{s} + 2\frac{s}{t} + 2 \right) + \frac{t^2}{s} + 2(s+t) \right] \ln\left(1 - \frac{z}{t}\right) \\
& + \left[\frac{z^2}{t} - 2z \left(1 + \frac{s}{t} \right) + 2\frac{t^2}{s} + 8s + 4\frac{s^2}{t} + 7t \right] \ln\left(1 - \frac{z}{t}\right) \ln\left(1 + \frac{t}{s}\right) + \left[\frac{z^2}{s} + 4z \left(1 + \frac{s}{t} \right) - \frac{t^2}{s} - 4(s+t) \right] \\
& \times \text{Li}_2\left(\frac{z}{t}\right) - \left[z^2 \left(\frac{1}{s} + \frac{1}{t} \right) + 2z \left(1 + \frac{s}{t} \right) + s + 2\frac{s^2}{t} \right] \text{Li}_2\left(-\frac{z}{s}\right) - \left[\frac{z^2}{t} - 2z \left(1 + \frac{s}{t} \right) + \frac{t^2}{s} + 5s + 2\frac{s^2}{t} + 4t \right] \\
& \times \text{Li}_2\left(1 + \frac{z}{u}\right) \} + 4c(s, t) \ln\left(\frac{2\omega}{\sqrt{s}}\right) \left[\ln\left(\frac{s}{m_e^2}\right) + \ln\left(-\frac{t}{s}\right) - \ln\left(1 + \frac{t}{s}\right) - 1 \right], \tag{9}
\end{aligned}$$

$$\begin{aligned}
F_2(z) = & \frac{1}{3} \left\{ 9c(t, s) \ln\left(\frac{s}{m_e^2}\right) - \left[z \left(\frac{t}{s} + \frac{s}{t} + 2 \right) - 5 \left(s + \frac{t}{2} + \frac{1}{2} \frac{s^2}{t} \right) \right] \ln\left(-\frac{t}{s}\right) - t \left(\frac{z}{s} - \frac{3}{2} \right) \right. \\
& \times \ln\left(1 + \frac{t}{s}\right) + \left[\frac{z^2}{2} \left(\frac{1}{s} + \frac{1}{t} \right) + z \left(1 + \frac{t}{s} \right) + 2\frac{t^2}{s} - \frac{s}{4} + \frac{3}{4}t \right] \ln^2\left(-\frac{t}{s}\right) \\
& - \left[\frac{z^2}{2s} - z \left(1 + \frac{t}{s} \right) + 2\frac{t^2}{s} + \frac{s^2}{t} + \frac{15}{4}s + \frac{9}{2}t \right] \ln^2\left(1 + \frac{t}{s}\right) - \left(4\frac{t^2}{s} + \frac{s^2}{t} + 4s + 5t \right) \ln\left(-\frac{t}{s}\right) \ln\left(1 + \frac{t}{s}\right) \\
& - 4 \left[2\frac{t^2}{s} + \frac{s^2}{t} + 3(s+t) \right] \left[1 + \text{Li}_2\left(-\frac{t}{s}\right) \right] \\
& + \left(12\frac{t^2}{s} + 3\frac{s^2}{t} + 12s + 15t \right) \zeta_2 - \left[2\frac{t^2}{s} + \frac{s^2}{t} + 3(s+t) \right] \ln\left(\frac{z}{s}\right) \left[\ln\left(1 + \frac{t}{s}\right) - \ln\left(-\frac{t}{s}\right) \right] \\
& + \left[z^2 \left(\frac{1}{t} + \frac{2}{s} + 2\frac{t}{s^2} \right) - z \left(\frac{s}{t} + 2 + 2\frac{t}{s} \right) \right] \ln\left(\frac{z}{s}\right) - \left[\frac{z^2}{t} + 4z \left(1 + \frac{t}{s} \right) - \frac{s^2}{t} - 4(s+t) \right] \text{Li}_2\left(1 - \frac{z}{s}\right) \\
& + \left[z^2 \left(\frac{1}{s} + \frac{1}{t} \right) + 2z \left(1 + \frac{t}{s} \right) + 2\frac{t^2}{s} + t \right] \text{Li}_2\left(1 + \frac{z}{t}\right) - \left[\frac{z^2}{s} - 2z \left(1 + \frac{t}{s} \right) + \frac{s^2}{t} + 2\frac{t^2}{s} + 4s + 5t \right] \\
& \times \text{Li}_2\left(1 + \frac{z}{u}\right) \} + 4c(t, s) \ln\left(\frac{2\omega}{\sqrt{s}}\right) \left[\ln\left(\frac{s}{m_e^2}\right) + \ln\left(-\frac{t}{s}\right) - \ln\left(1 + \frac{t}{s}\right) - 1 \right], \tag{10}
\end{aligned}$$

$$\begin{aligned}
F_3(z) = & \frac{1}{3} \left\{ \left[\frac{z^2}{s} - 2z \left(1 + \frac{t}{s} \right) + 4\frac{t^2}{s} + 2\frac{s^2}{t} + 7s + 8t \right] \ln\left(1 + \frac{t}{s}\right) - \left[z^2 \left(\frac{1}{s} + \frac{1}{t} \right) + 2z \left(1 + \frac{t}{s} \right) + 4\frac{t^2}{s} \right. \right. \\
& + \left. \frac{s^2}{t} + 3s + 4t \right] \ln\left(-\frac{t}{s}\right) - \left[z^2 \left(\frac{1}{t} + \frac{2}{s} + 2\frac{t}{s^2} \right) - 2z \left(2 + \frac{s}{t} + 2\frac{t}{s} \right) + \frac{s^2}{t} + 2(s+t) \right] \} \}, \tag{11}
\end{aligned}$$

$$\begin{aligned}
F_4(z) = & \frac{1}{3} \left\{ \left[\frac{z^2}{s} - 2z \left(1 + \frac{t}{s} \right) + 2\frac{t^2}{s} + 2\frac{s^2}{t} + \frac{11}{2}s + 5t \right] \ln\left(1 + \frac{t}{s}\right) \right. \\
& - \left[z^2 \left(\frac{1}{s} + \frac{1}{t} \right) + 2z \left(1 + \frac{t}{s} \right) + 2\frac{t^2}{s} + \frac{3}{2}s + \frac{5}{2}t \right] \ln\left(-\frac{t}{s}\right) - \left[z^2 \left(\frac{1}{t} + \frac{2}{s} + 2\frac{t}{s^2} \right) - 2z \left(2 + \frac{s}{t} + 2\frac{t}{s} \right) \right. \\
& \left. \left. - \frac{1}{2} \frac{s^2}{t} - s \right] \right\}. \tag{12}
\end{aligned}$$

As a by-product, we can easily get, from Eqns. (7) and (8), the $N_f = 2$ contributions from heavy fermion loop insertions, with the replacements $4M_\pi^2 \rightarrow 4m_f^2$, and $R_{\text{had}} \rightarrow R_f$.

Naturally, the predictions depend on R_{had} , which as we already stressed is based on experimental data. As we will shortly show, the size of the effects is relevant, but is small enough that only the leading digit matters. Therefore, the fine details and the use of older or more recent data sets will not change our conclusions. It turns out that, despite being used in many problems (like the muon anomalous magnetic moment for example), no recent fit of R_{had} is publicly available. For the purpose of estimating the effects, we decided to use an older version of R_{had} , as it was used in [11], which, however, has the advantage of being available by contacting the author [14]. It is expected that current data would not in-

duce changes larger than about 10% as far as the present analysis is concerned. Our numerical results are shown in two tables for typical small and large angles. For example, at small angles at LEP we obtain an additional correction of about 0.16% from the hadronic insertions \mathcal{C} , whereas at large angles at meson factories we get 0.05% to 0.32%. These and the other numbers have to be compared with the anticipated experimental accuracies varying from few tenths of per mille (at small angles e.g. at LEP or ILC/GigaZ) to few per mille at large angles (from meson factories to ILC) [15, 16, 17], which clearly makes them relevant. As a check on the consistency of the calculation it is interesting to note that the corrections show decoupling when the masses m_f^2 or M_π^2 become large compared to the kinematics. The exact electron loop contributions, shown here for comparison, are the largest, followed by the hadronic corrections. It is known that

\sqrt{s} [GeV]	1	10	M_Z	500
QED Born	440994	4409.94	53.0348	1.76398
ew. Born	440994	4409.95	53.0370	1.76331
self energies (A)	445283	4495.45	55.5352	1.90910
irred. vertices (B)	-56	-2.74	-0.1005	-0.00704
boxes+red. (C)	e	193	5.73	0.1357
	μ	< 1	0.42	0.0408
		—	0.08	0.0407
	τ	< 1	$< 10^{-2}$	0.0027
		—	—	-0.0096
	t	< 1	$< 10^{-2}$	$< 10^{-5}$
		—	—	—
	had	< 1	0.39	0.0877
$\sum_{\text{boxes+red.}} (C)$	193	6.54	0.2669	0.01860
A + B + C	445420	4499.25	55.7016	1.92066

TABLE I: Differential cross sections in nanobarns at a scattering angle $\theta = 3^\circ$, in units of 10^2 . A – QED α running [13]; B – irreducible vertex corrections, C – net sum of infrared-sensitive corrections, including double boxes, dispersion approach (first line) and analytical expansion [5] (second line). When $m_f^2 > s, |t|, |u|$, the entry is suppressed. Parameters: $\omega = \sqrt{s}/2$, $M_Z = 91.1876$ GeV, $m_t = 172.5$ GeV.

\sqrt{s} [GeV]	1	10	M_Z	500
QED Born	466537	4665.37	56.1067	1.86615
ew. Born	466558	4686.27	1289.3011	0.85496
self energies (A)	480106	4984.83	62.9027	2.17957
irred. vertices (B)	-494	-14.35	-0.4239	-0.02602
boxes + red. (C)	e	807	14.53	0.2706
	μ	160	6.08	0.1470
		153	6.08	0.1470
	τ	2	1.33	0.0752
		—	1.07	0.0752
	t	< 1	$< 10^{-2}$	0.0005
		—	—	-0.00013
	had.	234	16.07	0.4701
$\sum_{\text{boxes+red.}} (C)$	1203	38.01	0.9634	0.04880
A + B + C	480815	5008.49	63.4422	2.20235

TABLE II: The same as in Tab. I, at a scattering angle $\theta = 90^\circ$, in units of 10^{-4} .

the virtual corrections are partly compensated by soft real pair emission. The $\ln^3(s/m^2)$ terms from irreducible vertices get completely cancelled this way. Because the infrared sensible double boxes (combined with factorizable loop corrections and with real emission as described) are free of those spurious logarithms, it is not expected that their *order of magnitude* will be changed by adding

the emission of real fermion pairs (hadrons). Nevertheless, the (cut-dependent) evaluation of pair emission is a necessary next step.

Finally, we also compared the numerical results obtained here by dispersion relations (bold-face entries in tables) with the analytical results of [5], obtained in the limit of small fermion mass. In fact, the analytical results approach the dispersive ones in regions where the approximated analytical results become appropriate.

Summarizing, the virtual $N_f = 2$ corrections to Bhabha scattering amount typically to 0.1%. They have to be taken into account for precision studies, and a package for the evaluation is being made public at [12]. These corrections are dominated by the hadronic contributions. For the leptonic corrections, we agree with other computations. After combining the virtual corrections with the corresponding, cut-dependent real pair emissions, the numerical influence might become diminished, but not substantially. This may be best studied by improving the existing MC generators.

We would like to thank B. Kniehl and H. Burkhardt for help concerning R_{had} and A. Arbuzov, S.-O. Moch, and K. Mönig for discussions. Work supported in part by GGI and INFN in Florence, by SFB/TRR 9 of DFG, by the Sofja Kovalevskaja Programme of the Alexander von Humboldt Foundation, and by MRTN-CT-2006-035505 “HEPTOOLS” and MRTN-CT-2006-035482 “FLAVIANet”.

-
- [1] Z. Bern et al., *Phys. Rev.* **D63** (2001) 053007.
 - [2] A. Arbuzov et al., *Mod. Phys. Lett.* **A13** (1998) 2305; N. Glover et al., *Phys. Lett.* **B516** (2001) 33.
 - [3] A. Penin, *Phys. Rev. Lett.* **95** (2005) 010408.
 - [4] R. Bonciani et al., *Nucl. Phys.* **B716** (2005) 280.
 - [5] S. Actis et al., *Nucl. Phys.* **B786** (2007) 26.
 - [6] T. Becher and K. Melnikov, *JHEP* **06** (2007) 084.
 - [7] R. Bonciani et al., arXiv:0710.4775 [hep-ph].
 - [8] S. Actis et al., arXiv:0710.5111 [hep-ph].
 - [9] N. Cabibbo and R. Gatto, *Phys. Rev.* **124** (1961) 1577.
 - [10] F. Berends and G. Komen, *Phys. Lett.* **B63** (1976) 432.
 - [11] B. Kniehl et al., *Phys. Lett.* **B209** (1988) 337.
 - [12] DESY, webpage <http://www-zeuthen.desy.de/theory/>.
 - [13] S. Eidelman and F. Jegerlehner, *Z. Phys.* **C67** (1995) 585, and Fortran program hadr5n.f (2003).
 - [14] H. Burkhardt, TASSO-NOTE-192 (1981), and Fortran program repi.f (1986).
 - [15] K. Mönig, talk at Bhabha Workshop, Karlsruhe, April 2005, <http://sfb-tr9.particle.uni-karlsruhe.de/>.
 - [16] S. Jadach, talk at Bhabha Workshop, Karlsruhe, April 2005, <http://sfb-tr9.particle.uni-karlsruhe.de/>.
 - [17] G. Montagna, talk at XXXI Conf. “Matter to the Deepest”, Ustroń, Poland, Sept. 2007, <http://prac.us.edu.pl/~us2007/>.
 - [18] the kernels and related functions may be downloaded from [12].